Can We Consider Central Catadioptric Cameras and Fisheye Cameras within a Unified Imaging Model

Xianghua Ying and Zhanyi Hu*

National Laboratory of Pattern Recognition, Institute of Automation, Chinese Academy of Sciences, 100080 P.R.China
{xhying, huzy}@nlpr.ia.ac.cn,
http://nlpr-web.ia.ac.cn/English/rv/~ying/

Abstract. There are two kinds of omnidirectional cameras often used in computer vision: central catadioptric cameras and fisheye cameras. Previous literatures use different imaging models to describe them separately. A unified imaging model is however presented in this paper. The unified model in this paper can be considered as an extension of the unified imaging model for central catadioptric cameras proposed by Geyer and Daniilidis. We show that our unified model can cover some existing models for fisheye cameras and fit well for many actual fisheye cameras used in previous literatures. Under our unified model, central catadioptric cameras and fisheye cameras can be classified by the model's characteristic parameter, and a fisheye image can be transformed into a central catadioptric one, vice versa. An important merit of our new unified model is that existing calibration methods for central catadioptric cameras can be directly applied to fisheye cameras. Furthermore, the metric calibration from single fisheye image only using projections of lines becomes possible via our unified model but the existing methods for fisheye cameras in the literatures till now are all non-metric under the same conditions. Experimental results of calibration from some central catadioptric and fisheye images confirm the validity and usefulness of our new unified model.

1 Introduction

In many computer vision applications, including robot navigation, 3D reconstruction, and image-based rendering, a camera with a quite large field of view (FOV) is required. A conventional camera has a very limited field of view, therefore some omnidirectional cameras, such as cameras with fisheye lenses, multi-camera systems and catadioptric imaging systems are employed. There are some representative implementations of omnidirectional cameras described in [17]. In

* This work was supported by the National Key Basic Research and Development Program China (973) under grant No. 2002CB312104, and the National Natural Science Foundation China under grant No. 60121302.

T. Pajdla and J. Matas (Eds.): ECCV 2004, LNCS 3021, pp. 442–455, 2004.
© Springer-Verlag Berlin Heidelberg 2004

(a) (b)

Fig. 1. (a) An image from a central catadioptric camera which is combined a perspective camera with a hyperboloidal mirror, designed by the Center for Machine Perception, Czech Technical University, and its field of view is 217 degrees. (b) An image from a fisheye camera which is a Nikon COOLPIX 990 with FC-E8 fisheye lenses, and its FOV is 183 degrees. The two images are taken in almost same position and direction.

this paper, we will present a unified imaging model for catadioptric and fisheye cameras with single viewpoint constraint. A catadioptric camera is an imaging device which combines a pinhole and a reflective mirror. Baker and Nayar [1] derive the complete class of single-lens single-mirror catadioptric sensors which have a single effective viewpoint. A catadioptric camera with a single viewpoint is called central catadioptric camera. A fisheye camera is an imaging device which mounts a fisheye lens on a conventional camera. As noted in [4], fisheye cameras do not have a single projection center but a locus of projection centers called diacaustic. However, in many computer vision applications, such as robot navigation, image-based rendering etc., it is reasonable to assume that the small projection locus can be approximated by a single viewpoint if calibration accuracy under this assumption can satisfy the requirement of applications. Most existing literatures [3,5,6,7,8,10,14,15,19,20,22,24] use this assumption as well as this paper. Images taken from a central catadioptric camera and a fisheye camera are shown in Fig. 1a and 1b respectively.

The motivations for proposing a unified imaging model for central catadioptric and fisheye cameras are based on the following observations: Similar to that under central catadioptric cameras lines in space are projected into conics in the catadioptric image [18,21], we find that lines in space are also projected into conics in the fisheye image using Nikon FC-E8 fisheye lenses mounted on a Nikon COOLPIX 990. Smith et al. [20] claim that space lines are projected into conics using some fisheye camera if the fisheye camera satisfies a two-step model via a quadric surface. Bräuer-Burchardt and Voss [5] discover that the projections of space lines are circles under some fisheye cameras. Nene and Nayar [18] note that the projections of space lines are circles too under a central para-catadioptric camera. All these imply that there should exist a unified model for central catadioptric and fisheye cameras.

The unified imaging model for central catadioptric and fisheye cameras presented in this work is an extension of the unified imaging model for central catadioptric camera proposed by Geyer and Daniilidis [12]. We show that this new unified model can cover some existing models for fisheye camera [5,8,20] and fit well for many actual fisheye cameras used in [7,14,19,22,24]. The equivalence of different imaging models is rigorously proved. An important merit for proposing this new unified model is that calibration methods in [2,11,13,25] for central catadioptric cameras can be directly applied to fisheye cameras. Furthermore, the metric calibration from single fisheye image only using projections of lines becomes possible via our unified model whereas existing methods for fisheye cameras in [5,6,7,14,22] are all non-metric under the same conditions.

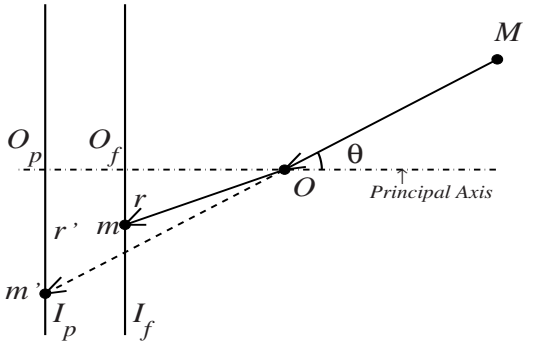

Fig. 2. Fisheye imaging process and its corresponding perspective projection. O is the projection center, I_p represents the perspective projection image plane, and I_f represents the fisheye image plane. For a space point M, its fisheye image is m and its perspective image is m'.

1.1 Related Work

There exists a unified imaging model for central catadioptric cameras proposed by Geyer and Daniilidis [12]. But for fisheye cameras, there exist many different imaging models in the literature. These existing models can be broadly divided into the following two categories:

1. Transformation between fisheye image and its corresponding perspective image

For a space point $\mathbf{M} = (X, Y, Z)^T$, let its fisheye image point $\mathbf{m} = (x, y)^T$, the corresponding perspective image point $\mathbf{m'} = (x', y')^T$, the origin of the world coordinate system located at the projection center, and the origins of the two image coordinate systems all located at the principal points (see Fig. 2). Therefore, we have $r = \sqrt{x^2 + y^2}$ and $r' = \sqrt{x'^2 + y'^2}$. The transformation between fisheye image and its corresponding perspective image can be represented by $(x, y) \overset{T}{\longleftrightarrow} (x', y')$ or $r \overset{T}{\longleftrightarrow} r'$. Basu et al. [3] present a logarithmic mapping

model, and Shah et al. [19] present a polynomial one. Recently, Bräuer-Burchardt et al. [5] and Fitzgibbon [8] propose a rational function model as:

$$r' = k_1 \frac{r}{1 - k_2 r^2}, \tag{1}$$

where k_1 and k_2 are two parameters of the model.

2. Transformation between fisheye image and its corresponding captured rays

The angle between a captured ray OM and the principle axis is denoted by θ(Fig. 2). The transformation between fisheye image and its corresponding captured rays is described as $(x, y) \overset{T}{\longleftrightarrow} \left(\frac{X}{\sqrt{X^2+Y^2+Z^2}}, \frac{Y}{\sqrt{X^2+Y^2+Z^2}}, \frac{Z}{\sqrt{X^2+Y^2+Z^2}}\right)$ or $r \overset{T}{\longleftrightarrow} \theta$. Xiong and Turkowski [24] present a polynomial model. Micusik and Pajdla [15] propose a rational function model. Miyamoto [16] uses equidistance projection model, and Fleck [10] employs stereographic projection model of the viewing sphere. Smith et al. [20] propose a two-step projection model via a quadric surface: the first step is that a 3D space point is projected to a point on the quadric surface which is the intersection of the captured ray with the quadric surface, and the second step is that the intersection point is orthographically projected to an image plane.

2 The Unified Imaging Model

In this section, we start with a generalized two-step projection model via a quadric surface, and then specify the generalized model in many different ways to obtain the unified imaging model and other two-step projection models. The proofs of the equivalence among these models are also provided in this section.

2.1 Generalized Two-Step Projection via a Quadric Surface (TSP0)

The generalized two-step projection is defined as follows: a space point is first projected to a point on the quadric surface, and then perspectively projected into a point on the image plane using a pinhole (see Fig. 3). There are some specific points about this generalized model:

1. The quadric surface is a revolution of a conic section about one of its principal axes where the foci lie. The effective viewpoint is located at one of the foci of the conic section and the pinhole lies on the revolution axis. Note that the pinhole can be located anywhere on the revolution axis. The image plane of the pinhole is perpendicular to the revolution axis. There are two different configurations with the different positions of the pinhole related to the quadric surface as shown in Fig. 3a and 3b.

2. The pinhole can be replaced by an orthographic camera. The quadric surface can be ellipsoidal ($0 < e < 1$, where e is the eccentricity of the conic section), paraboloidal ($e = 1$), hyperboloidal ($e > 1$) or some degenerated cases, such as, spherical ($e \to 0$) or planar ($e \to \infty$).

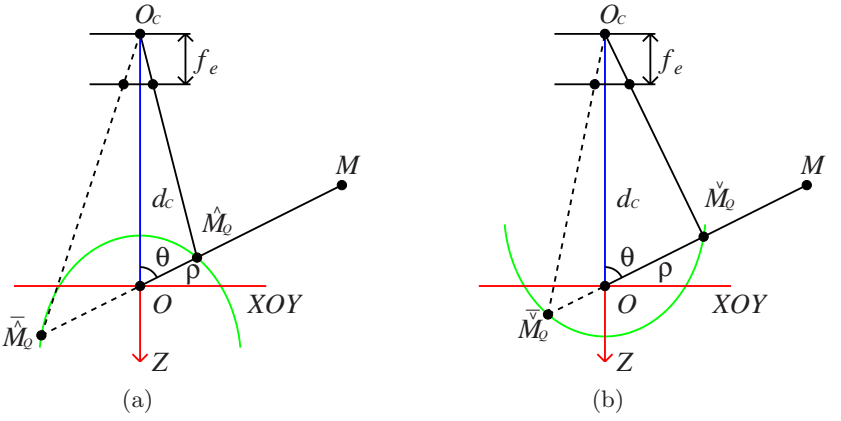

Fig. 3. A generalized two-step projection via a quadric surface. The effective viewpoint O is located at one of the foci of the quadric surface and the pinhole is located at O_C. A space point M is first projected into a point on the quadric surface, and then perspectively projected into a point on the image plane of the pinhole.

3. It is assumed that the quadric surface is transparent, i.e., the line OM intersects the quadric surface in two points. Note that the generalized two-step projection need not obey the law of reflection.

The world coordinate system $OXYZ$ is established as shown in Fig. 3. The origin of the coordinate system is located at the effective viewpoint O. The generalized projection of a space point $\mathbf{M} = (X, Y, Z)^T$ is denoted as:

$$(x, y) = Q_{e,p,f_e,d_c}(X, Y, Z), \tag{2}$$

where e is the eccentricity of the conic section, p is the distance from the focus to the directrix of the conic section, f_e is the effective focal length of the pinhole, and d_C is the distance from the origin to the pinhole. Because of the ambiguity caused by the transparence of the quadric surface and the position of the pinhole related to the quadric surface, there are four different projection points on the quadric surface: $\hat{M}_Q$, $\check{M}_Q$, $\bar{\hat{M}}_Q$ and $\bar{\check{M}}_Q$(see Fig. 3a and 3b). Hence, there are four different kinds of projections:

$$Q_{e,p,f_e,d_c} = \hat{Q}_{e,p,f_e,d_c} \cup \check{Q}_{e,p,f_e,d_c} \cup \bar{\hat{Q}}_{e,p,f_e,d_c} \cup \bar{\check{Q}}_{e,p,f_e,d_c}.$$

Because

$$\left(\bar{\hat{Q}}_{e,p,f_e,d_c} \cup \bar{\check{Q}}_{e,p,f_e,d_c}\right)(X, Y, Z) = \left(\hat{Q}_{e,p,f_e,d_c} \cup \check{Q}_{e,p,f_e,d_c}\right)(-X, -Y, -Z), \tag{3}$$

we will first find out $\hat{Q}_{e,p,f_e,d_c}$ and $\check{Q}_{e,p,f_e,d_c}$, and then derive $\bar{\hat{Q}}_{e,p,f_e,d_c}$ and $\bar{\check{Q}}_{e,p,f_e,d_c}$ using (3).

The ray OM intersects the quadric surface at $\hat{M}_Q$ in Fig. 3a (or $\check{M}_Q$ in Fig. 3b), the distance $O\hat{M}_Q$(or $O\check{M}_Q$) satisfies:

$$\rho = \frac{ep}{1 \pm e\cos\theta}, \tag{4}$$

where

$$cos\theta = -\frac{Z}{\sqrt{X^2+Y^2+Z^2}}. \tag{5}$$

$\hat{M}_Q$ (or $\check{M}_Q$) satisfies:

$$(X_Q, Y_Q, Z_Q) = \frac{\rho}{\sqrt{X^2+Y^2+Z^2}}(X, Y, Z), \tag{6}$$

where (X_Q, Y_Q, Z_Q) represents the world coordinates of $\hat{M}_Q$ (or $\check{M}_Q$). We assume the intrinsic matrix of the pinhole is:

$$\mathbf{K} = \begin{bmatrix} f_e & 0 & 0 \\ 0 & f_e & 0 \\ 0 & 0 & 1 \end{bmatrix}. \tag{7}$$

Therefore, the projection of $\hat{M}_Q$ (or $\check{M}_Q$) on the image plane satisfies:

$$\lambda\widetilde{\mathbf{m}} = \lambda \begin{bmatrix} x \\ y \\ 1 \end{bmatrix} = \begin{bmatrix} f_e & 0 & 0 \\ 0 & f_e & 0 \\ 0 & 0 & 1 \end{bmatrix} \begin{bmatrix} 1 & 0 & 0 & 0 \\ 0 & 1 & 0 & 0 \\ 0 & 0 & 1 & d_C \end{bmatrix} \begin{bmatrix} X_Q \\ Y_Q \\ Z_Q \\ 1 \end{bmatrix}, \tag{8}$$

where λ is an unknown scale factor, and $\widetilde{\mathbf{m}}$ is the homogeneous coordinates of $\mathbf{m} = (x, y)^T$. By eliminating λ from (8) and with (6), (4) and (5), we obtain:
$(x, y) = \left(\hat{Q}_{e,p,f_e,d_c} \cup \check{Q}_{e,p,f_e,d_c}\right)(X, Y, Z) =$

$$\left(\frac{epf_eX}{d_C\sqrt{X^2+Y^2+Z^2}+e(p \mp d_C)Z}, \frac{epf_eY}{d_C\sqrt{X^2+Y^2+Z^2}+e(p \mp d_C)Z}\right). \tag{9}$$

From (3) and (9), we obtain:
$(x, y) = \left(\bar{\hat{Q}}_{e,p,f_e,d_c} \cup \bar{\check{Q}}_{e,p,f_e,d_c}\right)(X, Y, Z) =$

$$\left(-\frac{epf_eX}{d_C\sqrt{X^2+Y^2+Z^2}-e(p \mp d_C)Z}, -\frac{epf_eY}{d_C\sqrt{X^2+Y^2+Z^2}-e(p \mp d_C)Z}\right). \tag{10}$$

2.2 Image Formation of Central Catadioptric Camera (TSP1)

Baker and Nayar [1] show that the only useful physically realizable mirror surfaces of catadioptric cameras that produce a single viewpoint are planar, ellipsoidal, hyperboloidal, and paraboloidal. For a planar mirror, given a fixed

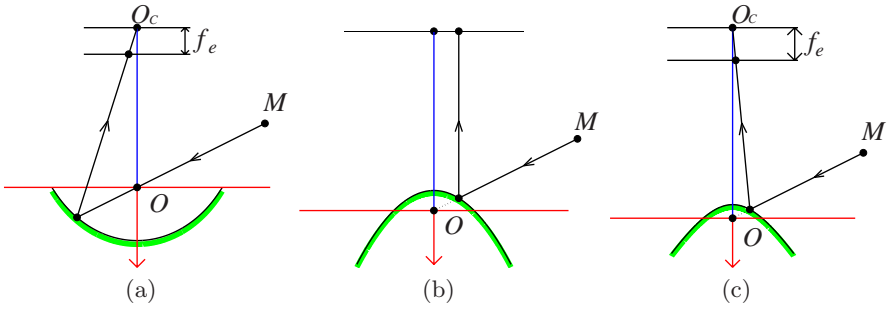

Fig. 4. Image formations of different kinds of central catadioptric cameras. (a) ellipsoidal, (b) paraboloidal, (c) hyperboloidal. Obviously, these models obey the law of reflection.

viewpoint and a pinhole, the configuration is the perpendicular bisector of the line joining the pinhole to the viewpoint. Under an orthographic camera, the only solution is a paraboloidal mirror with the effective viewpoint at the focus of the paraboloid. The hyperboloidal mirror satisfies the fixed viewpoint constraint when the pinhole and the viewpoint are located at the two foci of the hyperboloid. The ellipsoidal mirror can be configured in a similar way as the hyperboloidal one (see Fig. 4abc). Obviously, the four cases are all special cases of the generalized model. Since the planar catadioptric camera is equivalent to a pinhole, we do not discuss it here.

For the case of ellipsoid (see Fig. 4a), we have $0 < e < 1$ and $d_C = \frac{2e^2 p}{1-e^2}$(the distance of the two foci of the ellipsoid), then we obtain:

$$\begin{aligned}(x, y) &= E_{e,p,f_e}(X, Y, Z) = \bar{\tilde{Q}}_{e,p,f_e,d_c}(X, Y, Z) \\ &= \left(\frac{\frac{1-e^2}{1+e^2} f_e X}{-\frac{2e}{1+e^2}\sqrt{X^2+Y^2+Z^2}+Z}, \frac{\frac{1-e^2}{1+e^2} f_e Y}{-\frac{2e}{1+e^2}\sqrt{X^2+Y^2+Z^2}+Z} \right). \quad (11)\end{aligned}$$

For the case of paraboloid (see Fig. 4b), we have $e = 1$ and $f_e \to \infty, d_C \to \infty, \frac{f_e}{d_C} \to 1$. Since the paraboloidal has two ambiguous configurations, we obtain:

$$\begin{aligned}(x, y) &= P_p(X, Y, Z) = \left(\hat{Q}_{1,p,\infty,\infty} \cup \bar{\tilde{Q}}_{1,p,\infty,\infty} \right)(X, Y, Z) \\ &= \left(\mp \frac{pX}{-\sqrt{X^2+Y^2+Z^2}+Z}, \mp \frac{pY}{-\sqrt{X^2+Y^2+Z^2}+Z} \right). \quad (12)\end{aligned}$$

For the case of hyperboloid (see Fig. 4c), we have $e > 1$ and $d_C = \frac{2e^2 p}{1-e^2}$(the distance of the two foci of the hyperboloid), then we obtain:

$$\begin{aligned}(x, y) &= H_{e,p,f_e}(X, Y, Z) = \hat{Q}_{e,p,f_e,d_c}(X, Y, Z) \\ &= \left(\frac{\frac{1-e^2}{1+e^2} f_e X}{-\frac{2e}{1+e^2}\sqrt{X^2+Y^2+Z^2}+Z}, \frac{\frac{1-e^2}{1+e^2} f_e Y}{-\frac{2e}{1+e^2}\sqrt{X^2+Y^2+Z^2}+Z} \right). \quad (13)\end{aligned}$$

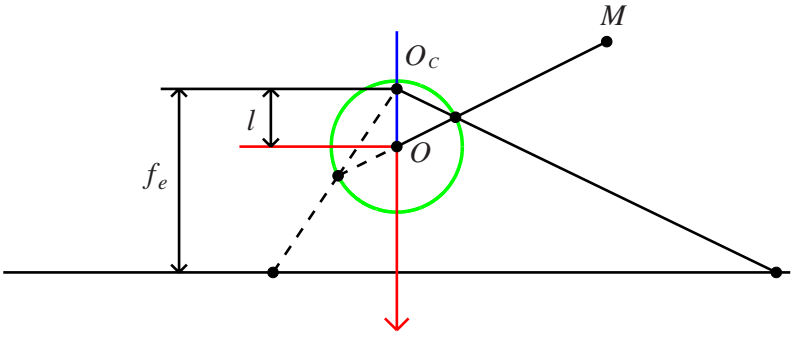

Fig. 5. A two-step projection via a unit sphere. O_C can lie inside, outside, or on the unit sphere.

2.3 Two-Step Projection via a Unit Sphere (TSP2)

The **TSP2** is the unified imaging model for central catadioptric and fisheye cameras. The reason for this will be given in Sect. 2.5. Obviously, the **TSP2** is a special case of the generalize model by setting $e \to 0, p \to \infty, ep \to 1$(see Fig. 5). If we let $d_C = l$, the projection can be represented as:

$$\begin{aligned}(x, y) &= S_{l,f_e}(X, Y, Z) = Q_{0,\infty,f_e,l}(X, Y, Z) = \left(\hat{Q} \cup \bar{\hat{Q}}\right)_{0,\infty,f_e,l}(X, Y, Z) \\ &= \left(\frac{f_e X}{\pm l\sqrt{X^2 + Y^2 + Z^2} + Z}, \frac{f_e Y}{\pm l\sqrt{X^2 + Y^2 + Z^2} + Z}\right). \end{aligned} \tag{14}$$

The unit sphere used here is called the viewing sphere. O_C can lie inside, outside, or on the viewing sphere. Note that this model has been proposed for central catadioptric cameras by Geyer and Daniilidis [12] where O_C is only inside, or on the viewing sphere.

2.4 Two-Step Projection via a Quadric Surface from an Orthographic Camera (TSP3)

The **TSP3** is a special case of the generalized model with $f_e \to \infty, d_C \to \infty, \frac{f_e}{d_C} \to 1$(see Fig. 6). The **TSP3** is also a special case of the model proposed in [20] where here we restrict that the quadric surface is a revolution of a conic section and the effective viewpoint is located at one of the foci of the conic section (Experimental results in Sect. 3 show that the special model with this restriction can also fit well for actual fisheye cameras). If we denote e as ε in order to avoid notational ambiguity where e has been used in the **TSP0** and **TSP1**, we can obtain:

$$\begin{aligned}(x, y) &= Q_{\varepsilon,p,\infty,\infty}(X, Y, Z) = \left(\hat{Q} \cup \check{Q} \cup \bar{\hat{Q}} \cup \bar{\check{Q}}\right)_{\varepsilon,p,\infty,\infty}(X, Y, Z) \\ &= \left(\pm\frac{pX}{\pm\frac{1}{\varepsilon}\sqrt{X^2 + Y^2 + Z^2} + Z}, \pm\frac{pY}{\pm\frac{1}{\varepsilon}\sqrt{X^2 + Y^2 + Z^2} + Z}\right). \end{aligned} \tag{15}$$

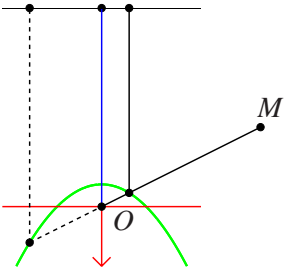

Fig. 6. A two-step projection via a quadric surface from an orthographic camera. The quadric surface can be ellipsoidal, paraboloidal, hyperboloidal, et al.

2.5 Equivalence among These Imaging Models

From (9) and (10) in Sect. 2.1, we know that the generalized model can be represented by a model with two parameters α, β:

$$\begin{aligned}(x, y) &= G_{\alpha,\beta}(X, Y, Z) \\ &= \left(\frac{\beta X}{\alpha\sqrt{X^2+Y^2+Z^2}+Z}, \frac{\beta Y}{\alpha\sqrt{X^2+Y^2+Z^2}+Z}\right),\end{aligned} \tag{16}$$

where $\alpha \in R, \beta \in R$ and $\beta \neq 0$. For the **TSP1**, from (11),(12) and (13) we obtain, $-1 \leq \alpha \leq 0 \cup \alpha = 1$ (for planar catadioptric camera, $e \to \infty, \alpha \to 0$). For the **TSP2**, from (14), we obtain $\alpha = \pm l$, obviously $\alpha \in R$ here. For the **TSP3**, from (15), we can obtain $\alpha = \frac{1}{\varepsilon}$. Let $\varepsilon \to \infty$, $\frac{1}{\varepsilon} \to 0$, and $\varepsilon \to 0$, $\frac{1}{\varepsilon} \to \infty$, then we obtain $\alpha \in R$.

Definition. $(x_1, y_1) = G_{\alpha_1,\beta_1}(X, Y, Z)$ and $(x_2, y_2) = G_{\alpha_2,\beta_2}(X, Y, Z)$ are two instances of the generalized two-step projection. If $\alpha_1 = \pm\alpha_2$ and $\beta_1 = s\beta_2 (s \in R, s \neq 0)$, we call that G_{α_1,β_1} and G_{α_2,β_2} are equivalent, and denoted by $G_{\alpha_1,\beta_1} \sim G_{\alpha_2,\beta_2}$.

From the above discussions, we have the following proposition for the equivalence among these models.

Proposition. $P_0/\sim = P_2/\sim = P_3/\sim \supset P_1/\sim$.
where P_i represents the set of all projections belong to **TSPi** (**i**=0,1,2,3), and $P_i/\sim$ represents the quotient set[1] of P_i.

Let us assume $l \geq 0$. The equivalence among **TSP1**, **TSP2** and **TSP3** are shown in Table 1. Therefore, we can let the **TSP2** as the unified imaging model for central catadioptric and fisheye cameras (the fitness of the unified model for actual fisheye cameras is illustrated by experimental results in Sect. 3). The parameter l is called the characteristic parameter of the unified model. Obviously, central catadioptric and fisheye cameras can be classified by the characteristic parameter. Note that Geyer and Daniilidis [12] have proved the equivalence between the **TSP1** and the **TSP2** when $0 \leq l \leq 1$.

[1] The set consisting of all equivalence classes of $\sim$.

Table 1. Equivalence among **TSP1**, **TSP2** and **TSP3**, see text for details

TSP1	**TSP2**	**TSP3**
Ellipsoidal $0 < e < 1$	Inside the viewing sphere $0 < l < 1$	Hyperboloidal $\varepsilon > 1$
Paraboloidal $e = 1$	On the viewing sphere $l = 1$	Paraboloidal $\varepsilon = 1$
Hyperboloidal $e > 1$	Inside the viewing sphere $0 < l < 1$	Hyperboloidal $\varepsilon > 1$
	Outside the viewing sphere $l > 1$	Ellipsoidal $0 < \varepsilon < 1$

For the case of $l = 0$, we obtain:

$$(x_0, y_0) = S_{0,f_{e0}}(X, Y, Z) = \left(f_{e0}\frac{X}{Z}, f_{e0}\frac{Y}{Z} \right). \tag{17}$$

It is a perspective projection and corresponds to a pinhole camera or a central planar catadioptric camera. For the case of $l = 1$, we obtain:

$$(x_1, y_1) = S_{1,f_{e1}}(X, Y, Z) = \left(\frac{f_{e1}X}{\sqrt{X^2 + Y^2 + Z^2} + Z}, \frac{f_{e1}Y}{\sqrt{X^2 + Y^2 + Z^2} + Z} \right). \tag{18}$$

It is the stereographic projection and equivalent to a central para-catadioptric camera, or some fisheye cameras such as those used in [5] and [8]. The reason for the equivalence of a central para-catadioptric camera can be known from (12). The reason for the equivalence of some fisheye camera will be derived below. From Fig. 2, we have:

$$r' = \sqrt{x_0^2 + y_0^2}, r = \sqrt{x_1^2 + y_1^2}. \tag{19}$$

From (17),(18) and (19), we obtain:

$$r' = 2\frac{f_{e0}}{f_{e1}} \frac{r}{1 - \frac{1}{f_{e1}^2} r^2}. \tag{20}$$

Obviously, (20) has the same form as (1).

3 Calibration

Under the unified imaging model, a line in space is projected to a conic in the image plane, and such a conic is called a line image. Since the unified imaging model is an extension of the unified imaging model for central catadioptric camera, the calibration methods for central catadioptric cameras using line images [2, 11,13,25] can be directly applied to fisheye cameras. These calibration methods for central catadioptric camera are all metric. Therefore, the metric calibration from single fisheye image only using projections of lines becomes possible via

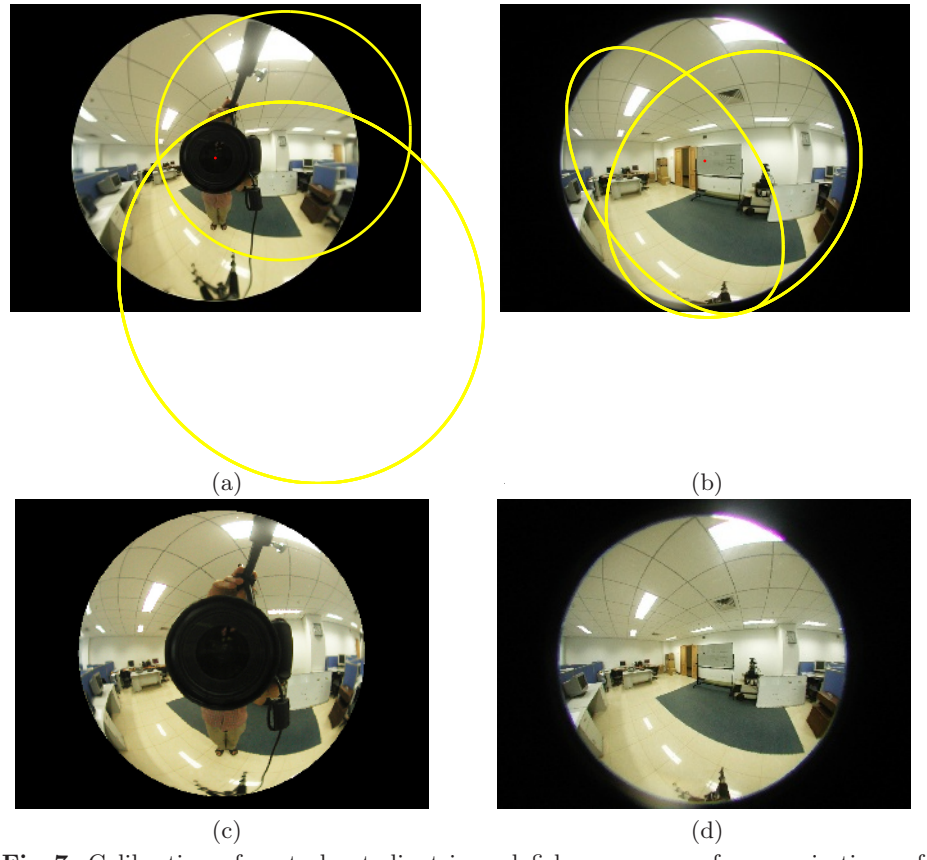

Fig. 7. Calibration of central catadioptric and fisheye cameras from projections of lines. (a) and (b) are conic fitting results for projections of lines from Fig. 1a and 1b. (c) and (d) are two synthesis images transformed from (a) and (b) respectively. The transformation from (a) to (c) is from catadioptric to fisheye, and the transformation from (b) to (d) is from fisheye to catadioptric. We can find that (a) and (d), (b) and (c) are almost the same (please compare the curvatures of corresponding projections of lines in these images). Note that the FOV of the catadioptric camera is larger than that of the fisheye camera.

our unified model but the existing methods for fisheye cameras in the literatures till now are all non-metric under the same conditions. Here, we use the calibration method based on the geometric invariants of line images proposed in [25], since the characteristic parameter l can be determined in an explicit form. Fig. 7 are some calibration results from the central catadioptric image and the fisheye image shown in Fig. 1a and 1b. Fig. 7a and 7b are conic fitting results for line images from Fig. 1a and 1b using some conic fitting methods [9,26]. Then we perform calibration using the method proposed in [25], and the intrinsic parameters of these cameras and the characteristic parameter l are obtained. The FOV of fisheye camera is also estimated at 189 ± 3.5 degrees which is very close to 183 degrees that provided by camera producer.

We know that the characteristic parameter l for central catadioptric cameras in the unified model is from 0 to 1, however we find the characteristic parameter l for some actual fisheye cameras is from 1 to infinite (for example, Nikon FC-E8 we used). Although the image formations with $0 < l < 1$ or $l > 1$ possess some similar properties, such as line images are conics, there are several different properties between them which are listed as follows: For central catadioptric camera with $0 < l < 1$, a line image can belong to any type of conic, namely, line, circle, ellipse, hyperbola and parabola, but for fisheye camera with $l > 1$, it can only be line, circle and ellipse. Another notable difference is that if a line image from central catadioptric camera is an ellipse, its major axis must pass through the image center. However if a line image from fisheye camera, its minor axis goes through the image center instead (see Fig. 7a and 7b).

Similar to central catadioptric image, we can determine the directions of captured lighting rays from fisheye image if the fisheye camera has been calibrated metrically. Examples of transformations between a fisheye image and a central catadioptric image based on the unified model are shown in Fig. 7cd. The transformation method used here is similar to the one proposed in [23]. Note that these transformations can be accomplished only after these images are metrically calibrated. We can find that Fig. 7a and 7d, Fig. 7b and 7c are almost same without noticeable difference except the FOV of the catadioptric camera is larger than that of the fisheye camera. Therefore, we can say that the results of metric calibration of the fisheye camera are comparable with those of the central catadioptric camera.

In order to validate the fitness of the unified model for many existing fisheye cameras, distortion correction procedures are performed for some fisheye images taken from previous publications [7,14,19,20,22,24]. We first calibrate fisheye cameras from these fisheye images, and then transform them into perspective ones. We find that distortion correction results using our unified model are comparable with those using existing models. All these demonstrate that the unified model fit well for these actual fisheye cameras.

4 Conclusions

We present a unified imaging model for central catadioptric and fisheye cameras. The unified imaging model is an extension of the unified imaging model for central catadioptric camera proposed by Geyer and Daniilidis. In order to prove the equivalence among imaging models, we present a generalized two-step projection via a quadric surface. Then other two-step projection models can be treated as the special cases of the generalized model. We show that the unified model can cover some existing models for fisheye camera, and fit well for many real fisheye cameras. The advantage of proposing the unified model is that many existing calibration methods for central catadioptric cameras can be directly applied to fisheye cameras. Furthermore, the metric calibration from single fisheye image only using projections of lines becomes possible with the unified model whereas the existing methods for fisheye cameras in the literatures till now are all non-metric under the same conditions.

References

1. S. Baker and S.K. Nayar, A Theory of Catadioptric Image Formation, In Proc. International Conference on Computer Vision, India, 1998, pp. 35–42
2. J.P. Barreto and H. Arajo, Geometric Properties of Central Catadioptric Line Images, In Proc. European Conference on Computer Vision, 2002, pp. 237–251
3. A. Basu and S. Licardie, Alternative models for fish-eye lenses, Pattern Recognition Letters, 16(4), 1995, pp. 433–441
4. M. Born and E. Wolf, Principles of Optics, Pergamon Press, 1965
5. C. Bräuer-Burchardt and K. Voss. A new algorithm to correct fish-eye- and strong wide-angle-lens-distortion from single images. In Proc. ICIP, pp. 225–228, 2001
6. D.C. Brown. Close range camera calibration. Photogrammetric Engineering, 37(8): pp.855–866, 1971
7. F. Devernay, O. Faugeras, Straight Lines Have to Be Straight: Automatic Calibration and Removal of Distortion from Scenes of Structured Environments, Machine Vision and Applications, 2001, vol.1, pp.14–24
8. A. Fitzgibbon. Simultaneous linear estimation of multiple view geometry and lens distortion. Proceedings of IEEE Conference on CVPR, 2001
9. A. Fitzgibbon, M. Pilu,R. Fisher, Direct least-square fitting of ellipses, ICPR, 1996
10. M.M. Fleck, Perspective Projection: the Wrong Imaging Model, technical report 95-01, Computer Science, University of Iowa, 1995
11. C. Geyer and K. Daniilidis, Catadioptric Camera Calibration. ICCV 1999: 398–404
12. C. Geyer and K. Daniilidis, A Unifying Theory for Central Panoramic Systems and Practical Implications, In Proc. ECCV, 2000, pp. 445–462
13. C. Geyer and K. Daniilidis, Paracatadioptric Camera Calibration, IEEE Transactions on Pattern Analysis and Machine Intelligence, 2002, 24(5): pp. 687–695
14. S. B. Kang, Radial distortion snakes, IAPR Workshop on MVA, 2000, pp. 603–606
15. B. Micusik and T. Pajdla, Estimation of Omnidirectional Camera Model from Epipolar Geometry, CVPR, 2003
16. K. Miyamoto. Fish eye lens. Journal of Optical Society of America, 54: pp. 1060–1061, 1964
17. S. K. Nayar, Omnidirectional Vision, Proc. of Eight International Symposium on Robotics Research, Shonan, Japan, October 1997
18. S.A. Nene and S.K. Nayar, Stereo with mirrors, In Proc. International Conference on Computer Vision, India, 1998, pp. 1087–1094
19. S. Shah, J. K. Aggarwal. Intrinsic Parameter Calibration Procedure for a (High Distortion) Fish-Eye Lens Camera with Distortion Model and Accuracy Estimation. Pattern Recognition, 1996, vol.29, no.11, pp. 1775–1788
20. P.W. Smith, K.B. Johnson, and M.A. Abidi, Efficient Techniques for Wide-Angle Stereo Vision using Surface Projection Models, CVPR, 1999
21. T. Svoboda, T. Padjla, and V. Hlavac, Epipolar geometry for panoramic cameras, In Proc. European Conference on Computer Vision, 1998, pp. 218–231
22. R. Swaminathan, S.K. Nayar. Non-Metric Calibration of Wide-Angle Lenses and Polycameras. PAMI, 2000, pp. 1172–1178
23. M. Urban, T. Svoboda, T. Pajdla, Transformation of Panoramic Images: from hyperbolic mirror with central projection to parabolic mirror with orthogonal projection, Technical report, The Center for Machine Perception, Czech Technical University, Prague, 2000
24. Y. Xiong, K. Turkowski. Creating Image-Based VR Using a Self-Calibrating Fisheye Lens. Proceedings of CVPR, 1997, 237–243

25. X. Ying, Z. Hu, Catadioptric Camera Calibration Using Geometric Invariants, International Conference on Computer Vision (ICCV2003), Nice, France, 2003
26. Z. Zhang, Parameter Estimation Techniques: A Tutorial with Application to Conic Fitting, INRIA Raport de Recherche n 2676, October 1995